Circuits Systems Signal Process
Vol. 18, No. 4, 1999, Pp. 331–350

# Stability Analysis for Rotating Stall Dynamics in Axial Flow Compressors*

*Guoxiang Gu,*[1] *Andrew Sparks,*[2] *and Calin Belta*[1]

**Abstract.** This paper analyzes the nonlinear phenomenon of rotating stall via the methods of projection [*Elementary Stability and Bifurcation Theory*, G. Iooss and D. D. Joseph, Springer-Verlag, 1980] and Lyapunov [J.-H. Fu, *Math. Control Signal Systems*, 7, 255–278, 1994]. A compressor model of Moore and Greitzer is adopted in which rotating stall dynamics are associated with Hopf bifurcations. Local stability for each pair of the critical modes is studied and characterized. It is shown that local stability of individual pairs of the critical modes determines collectively local stability of the compressor model. Explicit conditions are obtained for local stability of rotating stall which offer new insight into the design, and active control of axial flow compressors.

## 1. Introduction

Axial flow compressors are vital parts of the aeroengines. Yet two distinct aerodynamic instabilities, rotating stall and surge, can severely limit compressor performance. Both of these instabilities are disruptions of the normal operating condition, which is designed for steady and axisymmetric flow. Rotating stall is a severely nonaxisymmetric distribution of axial flow velocity around the annulus of the compressor, taking the form of a wave or *stall cell* that propagates steadily in the circumferential direction. Surge, on the other hand, is an axisymmetric oscillation of the mass flow along the axial length of the compressor. Both of these disruptions can have catastrophic consequences for jet airplanes.

* Received December 1997; revised November 1998. This research was supported in part by AFOSR and ARO.

An abridged version of this paper appeared in *Proceedings of the IEEE Conference on Decision and Control*, Tampa, FL, 1998.

[1]Department of Electrical and Computer Engineering, Louisiana State University, Baton Rouge, LA 70803-5901. E-mail: ggu@ee.lsu.edu

[2]Flight Dynamics Directorate, Wright Laboratory, Wright-Patterson Air Force Base, Ohio, 45433-7531.

The nonlinear phenomena of rotating stall and surge have been studied extensively in the literature in which a PDE (partial differential equation) model of Moore and Greitzer [10] becomes standard. In this PDE model, rotating stall dynamics are described by a PDE, and surge is described by two ODEs (ordinary differential equations). If only the fundamental harmonics in a spatial Fourier series of the disturbance flow is retained, the PDE model reduces to a third-order ODE model. The bifurcation phenomena associated with rotating stall and surge for this model are analyzed thoroughly in [2], [9].

Because the approximation error is due to the truncation of high-order harmonics in the disturbance flow, this paper will focus on stability analysis for rotating stall dynamics. The original PDE model of [10] will be investigated indirectly through transformation into an ODE model of order $2N + 2$, where $N \to \infty$ is the number of pairs of stall modes. This multimode model ($N > 1$) gives much more accurate representation and recovers the PDE model when $N \to \infty$. The equilibria of the uniform flow will be derived, and the rotating stall dynamics will be characterized for the multimode model. The local stability of the compressor model will be studied via both the methods of projection [7] and Lyapunov [3], for which necessary and sufficient conditions are obtained in terms of various compressor parameters.

Our results show that the stability condition for each pair of the critical modes determines the stability for rotating stall collectively. We point out that although in a special case our stability condition for rotating stall dynamics is the same as that for the simple third-order ODE model, stability analysis for the third-order ODE model cannot replace that for the PDE or for the multimode model. In fact, active control for rotating stall based on the third-order ODE model often fails to stabilize the critical operating point of the PDE model because of the neglected high-order harmonics in the disturbance flow.

Interested readers are referred to [4] for a more complete reference on stability and stabilization of the rotating stall dynamics for the third-order Moore-Greitzer model. Our stability analysis for the multimode model with $N \to \infty$ and the explicit conditions for local stability of rotating stall offer new insight into the design, and active control for axial flow compressors.

A schematic axial flow compressor is shown in Figure 1. The following notation is used in this paper:

| | | | |
|---|---|---|---|
| $R =$ | mean rotor radius | $l_c =$ | $l_I + l_E + 1/a$ |
| $A_c =$ | compressor duct area | $V_p =$ | volume of plenum |
| $U =$ | blade speed at mean radius | $\mu =$ | viscosity coefficient |
| $a_s =$ | speed of sound | $p_S =$ | static pressure in plenum |
| $B =$ | $(U/2a_s)\sqrt{V_p/(A_c L c)}$ | $p_T =$ | total pressure ahead of entrance |
| $W =$ | semiwidth of cubic characteristic | | and following the throttle duct |
| $a, b =$ | time lag of blade passage | $\Psi =$ | $(p_S - p_T)/\rho U^2$: pressure rise |

| | | | |
|---|---|---|---|
| $H =$ | semiheight of cubic characteristic | $\phi =$ | local flow coefficient at station 0 |
| $\gamma =$ | throttle position | $\Phi =$ | mean flow coefficient at station 0 |
| $m =$ | exit duct length factor | $\varphi =$ | disturbance flow at $\eta$ |
| $l_E, l_I, l_T =$ | length of exit, entrance, throttle ducts, in wheel radius | $\eta =$ | axial distance from station 0 |
| | | $\xi =$ | $Ut/R$ where $t$ is time |

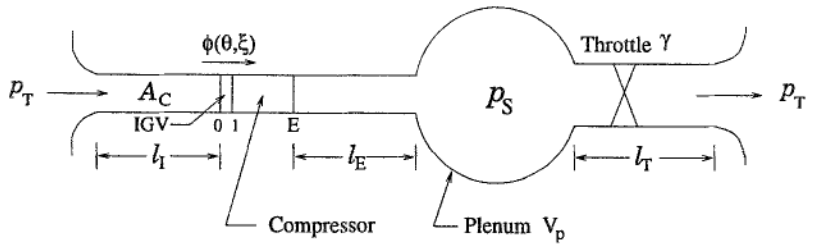


**Figure 1.** Schematic of compressor showing nondimensionalized lengths.

## 2. Multimode Moore-Greitzer model

A post-stall model for compression systems was developed by Moore and Greitzer. Its full PDE form is described by [10]

$$\Psi + l_c \frac{d\Phi}{d\xi} = \psi_c(\phi) - m\left(\frac{\partial}{\partial \xi}\int_{-l_F}^{0} \varphi \, d\eta\right) - \left(\frac{1}{a}\frac{\partial \varphi}{\partial \xi} + \frac{1}{b}\frac{\partial \varphi}{\partial \theta} - \mu \frac{\partial^2 \varphi}{\partial \theta^2}\right)\Bigg|_{\eta=0}, \tag{1}$$

$$\dot{\Psi} = \frac{1}{4B^2 l_c}\left(\Phi - \gamma\sqrt{\Psi}\right), \tag{2}$$

where $\phi = \Phi + \varphi|_{\eta=0}$ is the local mass flow at station 0. The incompressible and irotational assumption on the gas flow implies the existence of a disturbance flow potential that satisfies Laplace's equation with zero boundary condition at $\eta = -l_F \leq -l_c$, which in turn implies that the disturbance flow at station 0 has the form:

$$\varphi|_{\eta=0} = \sum_{n=1}^{N} (A_n \cos(n\theta) + B_n \sin(n\theta)), \quad N \to \infty. \tag{3}$$

Let $\{e^{j\theta_n}\}_{n=0}^{2N}$ be a set of $2N + 1$ uniformly distributed samples on the unit circle. Denote

$$\phi_N^{\mathrm{T}} = [\,\phi(\theta_1) \quad \phi(\theta_2) \quad \cdots \quad \phi(\theta_{2N+1})\,], \tag{4}$$

$$T = \sqrt{\frac{2}{2N+1}} \begin{bmatrix} \frac{1}{\sqrt{2}} & \frac{1}{\sqrt{2}} & \cdots & \frac{1}{\sqrt{2}} \\ \cos\theta_1 & \cos\theta_2 & \cdots & \cos\theta_{2N+1} \\ \sin\theta_1 & \sin\theta_2 & \cdots & \sin\theta_{2N+1} \\ \vdots & \vdots & \ddots & \vdots \\ \cos N\theta_1 & \cos N\theta_2 & \cdots & \cos N\theta_{2N+1} \\ \sin N\theta_1 & \sin N\theta_2 & \cdots & \sin N\theta_{2N+1} \end{bmatrix}, \tag{5}$$

$$E = \operatorname{diag}(l_c, m_1 I_2, m_2 I_2, \ldots, m_N I_2), \tag{6}$$

$$m_n = \frac{m\cosh(nl_F)}{n\sinh(nl_F)} + \frac{1}{a}, \qquad I_2 = \begin{bmatrix} 1 & 0 \\ 0 & 1 \end{bmatrix}, \tag{7}$$

$$F = \operatorname{diag}\left(0, \begin{bmatrix} -\mu & -\frac{1}{b} \\ \frac{1}{b} & -\mu \end{bmatrix}, \ldots, \begin{bmatrix} -\mu N^2 & -\frac{N}{b} \\ \frac{N}{b} & -\mu N^2 \end{bmatrix}\right), \tag{8}$$

$$M_1 = T^{\mathrm{T}} E^{-1} F T \quad M_2 = T^{\mathrm{T}} E^{-1} T. \tag{9}$$

Then the full PDE model can be approximated by the following multimode Moore-Greitzer model [8]:

$$\dot{\phi}_N = M_1\phi_N + M_2\psi_c(\Delta\phi_N) - M_2\bar{e}_n\Psi, \quad \Delta\phi_N = \frac{\phi_N}{W} - \bar{e}_N, \tag{10}$$

$$\dot{\Psi} = \frac{1}{4B^2 l_c}\left(\frac{\bar{e}_N^{\mathrm{T}}\phi_N}{2N+1} - \gamma\sqrt{\Psi}\right), \quad \bar{e}_N^{\mathrm{T}} = [\,1 \quad 1 \quad \cdots \quad 1\,]. \tag{11}$$

This multimode model converges to the PDE model described in (1) and (2) uniformly as $N \to \infty$ under some rather mild assumptions. Note that $T^{-1} = T^{\mathrm{T}}$, and

$$T\bar{e}_N = e_N\sqrt{2N+1}, \qquad T^{\mathrm{T}}e_N = \frac{\bar{e}_N}{\sqrt{2N+1}}, \tag{12}$$

and $e_N^{\mathrm{T}} = [\,1 \quad 0 \quad \cdots \quad 0\,]$. The performance characteristic curve $\psi_c(\cdot)$ is assumed to be a cubic polynomial [10] and is given by

$$\psi_c(\phi_N) = H\left[c_0\bar{e}_N + c_1\phi_N + c_3\phi_N^{\cdot 3}\right], \tag{13}$$

where $x^{\cdot 2} = x^{\cdot k}\big|_{k=2} = x \cdot x$ denotes a Hadamard product [5], where $x^{\cdot k}$ raises each element of $x$ to the power of $k$. The uniform flow can be represented by $\phi_N = \phi_e\bar{e}_N$, where $\phi_e$ is the intensity of the flow rate.

Suppose that the flow is perturbed near the equilibria of the uniform flow. Then

$$\phi_N = \phi_e\bar{e}_N + \delta\phi_N, \quad \Delta\phi_N = \frac{1}{W}\delta\phi_N + \left(\frac{\phi_e}{W} - 1\right)\bar{e}_N, \tag{14}$$

where $\phi_e \neq 0$ is a scalar factor, representing the flow rate intensity. It follows that

$$\delta\dot{\phi}_N = \left(M_1 + M_2 H\left[\frac{c_1}{W} + \frac{3c_3}{W}\left(\frac{\phi_e}{W} - 1\right)^2\right]\right)\delta\phi_N + \frac{3Hc_3}{W^2}\left(\frac{\phi_e}{W} - 1\right)M_2\delta\phi_N^{\cdot 2} + \frac{Hc_3}{W^3}M_2\delta\phi_N^{\cdot 3}$$

$$+\left(M_1\phi_e + M_2 H\left[c_0 + c_1\left(\frac{\phi_e}{W} - 1\right) + c_3\left(\frac{\phi_e}{W} - 1\right)^3\right]\right)\bar{e}_N - M_2\bar{e}_N\Psi. \tag{15}$$

**Proposition 2.1.** *The steady equilibria* $(\phi_N, \Psi) = (\phi_e\bar{e}_N, \Psi_e)$ *for the multimode compressor model of (10) and (11) are dependent on the throttle position parameter* $\gamma$ *and are governed by*

$$\Psi_e = H\left[c_0 + c_1\left(\frac{\phi_e}{W} - 1\right) + c_3\left(\frac{\phi_e}{W} - 1\right)^3\right] = \frac{\phi_e^2}{\gamma^2}. \tag{16}$$

**Proof.** Consider the perturbed multimode model for $\phi_N = \phi_e\bar{e}_N + \delta\phi_N$. Then $\delta\phi_N = 0$ is an equilibrium if and only if there exists a real $\Psi_e$ such that

$$\left(M_1\phi_e + M_2 H\left[c_0 + c_1\left(\frac{\phi_e}{W} - 1\right) + c_3\left(\frac{\phi_e}{W} - 1\right)^3\right]\right)\bar{e}_N - M_2\bar{e}_N\Psi_e = 0. \tag{17}$$

Denote $I_k$ as the identity matrix of size $k$. Substituting the expressions of $M_1$ and $M_2$ gives

$$T^{\mathrm{T}}E^{-1}\left(F\phi_e + H\left[c_0 + c_1\left(\frac{\phi_e}{W} - 1\right) + c_3\left(\frac{\phi_e}{W} - 1\right)^3\right]I_{2N+1} - \Psi_e I_{2N+1}\right)e_N = 0. \tag{18}$$

Because the (1-1)-position of $F$ is zero, this equation is equivalent to the first equality in (16). By setting $\dot{\Psi} = 0$, the equilibrium point $\Psi_e$ has to satisfy an additional condition,

$$\gamma\sqrt{\Psi_e} = \frac{\bar{e}_N^{\mathrm{T}}}{2N+1}\phi_e\bar{e}_N = \phi_e, \tag{19}$$

which is equivalent to the second equality of (16). Hence (16) characterizes the equilibria of the compressor model. □

Proposition 2.1 indicates that the equilibria of the multimode model are functions of $\gamma$, the throttle parameter, which can in turn be determined by the equilibria as in (19). Equation (19) is also referred to as the throttle curve as shown in Figure 2 (the dashed lines A-B and C-D for two different $\gamma$ values).

Denote the state variable as $x = \delta\phi_N \oplus \delta\Psi$ where $\oplus$ denotes the direct sum and $\delta\Psi = \Psi - \Psi_e$. A local model around the equilibria $(\phi_e\bar{e}_N, \Psi_e)$ has the form

$$\dot{x} = f(\gamma, x) = Lx + Q[x, x] + C[x, x, x] + \cdots, \tag{20}$$

where

$$L = S^{-1}\begin{bmatrix} \tau & \kappa e_N^{\mathrm{T}} \\ -\kappa e_N & E^{-1/2}(F+\alpha I)E^{-1/2} \end{bmatrix} S, \tag{21}$$

$$Q[x,x] = \begin{bmatrix} \frac{3Hc_3}{W^2}\left(\frac{\phi_e}{W}-1\right)M_2 & 0_{2N+1} \\ 0_{2N+1}^{\mathrm{T}} & -\frac{\tau}{4\Psi_e} \end{bmatrix} x^{\cdot 2}, \tag{22}$$

$$C[x,x,x] = \begin{bmatrix} \frac{Hc_3}{W^3}M_2 & 0_{2N+1} \\ 0_{2N+1}^{\mathrm{T}} & \frac{\tau}{8\Psi_e^2} \end{bmatrix} x^{\cdot 3}. \tag{23}$$

In the preceding expressions,

$$S = \begin{bmatrix} 0 & 2B\sqrt{(2N+1)l_c} \\ E^{1/2}T & 0 \end{bmatrix}, \tag{24}$$

$$\kappa = \frac{1}{2Bl_c}, \quad \tau = -\frac{\gamma}{8B^2 l_c\sqrt{\Psi_e}}, \tag{25}$$

$$\alpha = H\psi_c' = H\frac{d\psi_c}{d\phi_e} = \frac{H}{W}\left[c_1 + 3c_3\left(\frac{\phi_e}{W}-1\right)^2\right]. \tag{26}$$

By the form of $e_N$, the linear matrix can be written as

$$L = S^{-1}DS, \quad D = \mathrm{diag}\,(D_0, D_1, \cdots, D_N), \tag{27}$$

$$D_0 = \begin{bmatrix} \tau & \kappa \\ -\kappa & \alpha/l_c \end{bmatrix}, \quad D_n = \begin{bmatrix} \alpha-\mu n^2 & -n/b \\ n/b & \alpha-\mu n^2 \end{bmatrix} m_n^{-1}, \tag{28}$$

for $1 \le n \le N$. Because $S$ is a matrix of similarity transformation, an eigenvalue $\lambda$ of $L$ satisfies

$$\det\begin{bmatrix} \lambda-\tau & -\kappa e_N^{\mathrm{T}} \\ \kappa e_N & \lambda I - E^{-1/2}(F+\alpha I)E^{-1/2} \end{bmatrix} = 0.$$

**Proposition 2.2.** *Consider the compressor model of (10) and (11). Its linearized system near $(\phi_e \bar{e}_N, \Psi_e)$ as in (16) has $(N+1)$ pairs of eigenvalues that are given as follows:*

$$\lambda_{1,2} = 0.5(\tau+\alpha/l_c) \pm 0.5j\sqrt{4(\kappa^2+\tau\alpha/l_c) - (\tau+\alpha/l_c)^2}, \tag{29}$$

$$\lambda_{2n+1,2n+2} = \left(\alpha - \mu n^2 \pm j\frac{n}{b}\right)m_n^{-1}, \tag{30}$$

*where $n = 1, 2, \ldots, N$, and $j = \sqrt{-1}$.*

**Proof.** Careful observation of $SLS^{-1}$ with $L$ and $S$ as given in (21) yields

$$D = SLS^{-1} = \mathrm{diag}(D_0, D_1, \ldots, D_N), \qquad D_0 = \begin{bmatrix} \tau & \kappa \\ -\kappa & \alpha/l_c \end{bmatrix}, \tag{31}$$

$$D_n = \begin{bmatrix} \alpha-\mu n^2 & -n/b \\ n/b & \alpha-\mu n^2 \end{bmatrix} m_n^{-1}, \qquad n = 1, 2, \cdots, N. \tag{32}$$

Direct calculation for the eigenvalues of $L$ gives

$$\det(\lambda I - L) = \det(\lambda I - D) = \prod_{n=0}^{N} \det(\lambda I - D_n) = 0,$$

$$\Longleftrightarrow \det(\lambda I - D_0) = \lambda^2 - (\tau + \alpha/l_c)\lambda + \kappa^2 + \tau\alpha/l_c = 0,$$

$$\det(\lambda I - D_n) = (m_n\lambda - \alpha + \mu n^2)^2 + n^2/b^2 = 0.$$

Hence the expressions for $2(N + 1)$ eigenvalues of $L$ are those shown in (29) and (30). □

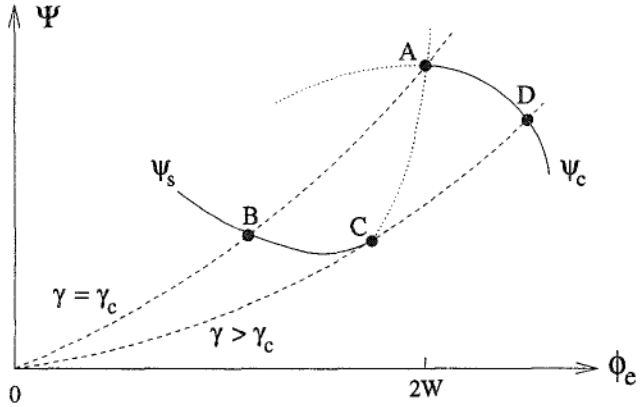


**Figure 2.** Schematic compressor characteristic, showing rotating stall.

Let us first examine the performance curve $\psi_c(\cdot)$ for the special case of $\mu = 0$. See the A-D curve in Figure 2, where the dashed lines are the throttle curve $\Psi_e = \phi_e^2/\gamma^2$, whose intersection with $\psi_c(\cdot)$ determines the operating point. The maximum pressure rise takes place at $\alpha = 0$ (point A), where the derivative of $\psi_c(\cdot)$ equals zero. Because $\alpha < 0$ on the right side of the maximum pressure rise, the $N$ pairs of eigenvalues of the $L$ matrix as given in (30) are stable. By $\tau < 0$ the pair of eigenvalues of (29) are also stable. Hence the compressor model is locally stable at the right of point A, and the axisymmetric flow $\phi_N = \phi_e \bar{e}_N$ is a stable equilibrium. However, if the throttle value $\gamma$ decreases, then the flow rate intensity $\phi_e$ decreases, and the derivative of $\psi_c(\cdot)$ eventually becomes positive. Thus the compressor model is unstable at the left of point A. In this case the $N$ pairs of eigenvalues in (30) cross the imaginary axis simultaneously. This is called the *critical case*, for which Hopf bifurcations occur that induce rotating stall. For $N = 1$, the compressor operates along the stall curve $\psi_s(\cdot)$, as shown in the B-C branch of Figure 2 which is locally stable. If the underlying bifurcations are subcritical, or unstable, the A-C portion of the stall curve is unstable. Stall cells will be born at point A and will grow, which will throttle the operating point from A to B quickly. There is a tremendous drop in both the pressure rise and the flow rate. Moreover, increasing the throttle position and flow rate at point B does not

increase the pressure rise. Rather, the pressure rise becomes even lower before it reaches point C, at which it jumps back to (again because of loss of stability) the performance curve $\psi_c(\cdot)$. The hysteresis loop A-B-C-D is the main cause of loss of compressor performance and potential damage to aeroengines. On the other hand, if the underlying bifurcations are stable, or supercritical, then point A represents a stable equilibrium. Decreasing the flow rate will not throttle the operating point to B. For $N = 1$, the pressure rise will gradually decrease along the curve A-C (which will be above the throttle line at $\gamma = \gamma_c$) and can thus be easily reversed by increasing the throttle position. Hence the stability of the Hopf bifurcation plays an important role in analyzing the stability of the rotating stall dynamics.

For the case $\mu > 0$, the critical value of the flow rate intensity $\phi_e$ takes place on the left of the maximum pressure rise because the viscosity coefficient $\mu$ tends to damp out the flow instability, thus delaying the occurrence of rotating stall. A further decrease in the flow rate intensity will also cause instability of the pair of eigenvalues in (29) that corresponds to surge dynamics. The next result characterizes the critical throttle parameter corresponding to rotating stall.

**Corollary 2.3.** *Suppose that $c_1 + 3c_3 = 0$ for the performance characteristic curve $\psi_c(\cdot)$, and $\mu = 0$. Then the N pairs of eigenvalues as in (30) cross the imaginary axis at the same critical throttle parameter value*

$$\gamma = \gamma_c = \left.\frac{\phi_e}{\sqrt{\Psi_e}}\right|_{\phi_e = 2W} = \frac{2W}{\sqrt{\psi_c(2W)}} = \frac{2W}{\sqrt{H(c_0 + c_1 + c_3)}}, \tag{33}$$

*and $\lambda_{2n+1,2n+2} = \pm j\frac{n}{b}m_n^{-1}$ for $1 \le n \le N$. For $\mu > 0$, the N pairs of eigenvalues as in (30) cross the imaginary axis at N different critical throttle parameter values that are given by*

$$\gamma = \gamma_{c_n} = \frac{W\left(1 + \sqrt{1 + \frac{\mu n^2 W}{3Hc_3}}\right)}{\left[Hc_0 + Hc_1\sqrt{1 + \frac{\mu n^2 W}{3Hc_3}} + Hc_3\left(\sqrt{1 + \frac{\mu n^2 W}{3Hc_3}}\right)^3\right]^{1/2}}, \tag{34}$$

*and expression $\lambda_{2n+1,2n+2} = \pm j\frac{n}{b}m_n^{-1}$ remains the same for $n = 1, 2, \ldots, N$.*

**Proof.** Because $c_1 + 3c_3 = 0$, $\phi_e = 2W$ is the critical flow rate intensity if $\mu = 0$. Substituting into (16) and (19) yields the critical throttle parameter value as in (33). For $\mu \neq 0$, the $n$th pair of eigenvalues cross the imaginary axis at $\alpha = \mu n^2$, or

$$\frac{\phi_e}{W} - 1 = \sqrt{1 + \frac{\mu n^2 W}{3Hc_3}}. \tag{35}$$

Substituting into (16) yields the critical throttle parameter value as in (34). □

For $\mu > 0$, the largest $N$ value such that $\gamma_{c_n}$ is real for $n = 1, 2, \ldots, N$ is bounded as $N \leq \sqrt{-3c_3H/(\mu W)}$. This is the same as in [2].[3] For $\mu = 0$, the largest $N$ value can be unbounded. Moreover the critical values of $\phi_e$ and $\Psi_e$ under the condition of $c_1 + 3c_3 = 0$ are given by

$$\phi_c = 2W, \quad \Psi_c = H(c_0 + c_1 + c_3). \tag{36}$$

## 3. Stability analysis for rotating stall

This section considers rotating stall dynamics with $N$ pairs of critical modes corresponding to $N$ harmonics of spatial Fourier series for the local flow rate. Local stability for each pair of the critical modes will be analyzed first using the projection method [7], [6] (as outlined in the Appendix). It is known that even if every pair of critical modes corresponding to the rotating stall is stable, the rotating stall dynamics still may not be stable because of the coupling of different pairs of critical modes. Hence the Lyapunov method of Fu [3] (as outlined in the Appendix) will be adopted to analyze further the local stability of the rotating stall. It will be demonstrated that for the case of $\mu = 0$, local stability of each pair of the critical modes implies local stability of the rotating stall dynamics.

From Section 2, a local model of the multimode Moore-Greitzer model has the form in (20), where linear, quadratic, and cubic terms are given as in (21) through (23). In order to apply the projection and the Lyapunov method, left and right critical eigenvectors corresponding to the rotating stall must be computed. Denote $\Theta_n$ as a column vector of size $2N + 1$ as

$$\Theta_n = [\, e^{-jn\theta_1} \quad e^{-jn\theta_2} \quad \cdots \quad e^{-jn\theta_{2N+1}} \,]^{\mathrm{T}}, \tag{37}$$

where the $e^{j\theta_k}$'s are equally distributed on the unit circle as assumed.

**Lemma 3.1.** *The right and left eigenvectors corresponding to the nth pair of the critical eigenvalues associated with rotating stall are given by*

$$r_n = \sqrt{\frac{2m_n^{-1}}{2N+1}}\,[\,1 \quad j\,]\,u_n \begin{bmatrix} \Theta_n \\ 0 \end{bmatrix}, \quad \ell_n = \sqrt{\frac{2m_n}{2N+1}}\,u_n^{\mathrm{T}} \begin{bmatrix} 1 \\ -j \end{bmatrix} [\,\Theta_n^{\mathrm{H}} \quad 0\,], \tag{38}$$

*respectively, for $1 \leq n \leq N$, where $u_n$ is an arbitrary nonzero column vector of size 2. Moreover, $\ell_n r_n = 1$ if and only if $\|u_n\| = \sqrt{u_n^{\mathrm{T}} u_n} = 1/\sqrt{2}$.*

**Proof.** See the Appendix. □

[3] Actually the $\mu$ parameter in [2] is different from what we used here. Taking $\mu \to \mu/(2a)$ will then give exactly the same expression as in [2].

With $r_n$ as in Lemma 3.1, $(r_n \cdot r_n = r_n^{\cdot 2})$, $(r_n \cdot \bar{r}_n) = |r_n|^{\cdot 2}$, and $(r_n \cdot r_n \cdot \bar{r}_n)$ are given by

$$r_n^{\cdot 2} = \frac{p_n^2}{2}\begin{bmatrix}\Theta_{2n}\\ 0\end{bmatrix}e^{2j\delta_n},\quad p_n = \sqrt{\frac{2m_n^{-1}}{2N+1}},\quad \delta_n = \tan^{-1}\left(\frac{u_{n2}}{u_{n1}}\right),\quad u_n = \begin{bmatrix}u_{n1}\\ u_{n2}\end{bmatrix}, \tag{39}$$

$$|r_n|^{\cdot 2} = \frac{p_n^2}{2}\begin{bmatrix}\bar{e}_N\\ 0\end{bmatrix},\quad r_n \cdot r_n \cdot \bar{r}_n = \frac{p_n^3}{2\sqrt{2}}\begin{bmatrix}\Theta_n\\ 0\end{bmatrix}e^{j\delta_n} = \frac{p_n^2 r_n}{2}. \tag{40}$$

To determine the stability of the $n$th pair of the critical modes corresponding to rotating stall, column vectors $\mu_n$ and $\nu_n$ as defined in (75) must be computed. It is noted that

$$\begin{aligned} SQ_0[r_n, \bar{r}_n] &= \frac{p_n^2}{2}\begin{bmatrix}0_{2N+1}^{\mathrm{T}} & 2B\sqrt{(2N+1)l_c}\\ E^{1/2}T & 0\end{bmatrix}\\ &\qquad \times \begin{bmatrix}\frac{3Hc_3}{W^2}\left(\frac{\phi_c}{W}-1\right)T^{\mathrm{T}}E^{-1}T & 0_{2N+1}\\ 0_{2N+1}^{\mathrm{T}} & -\frac{\tau}{4\Psi_c}\end{bmatrix}\begin{bmatrix}\bar{e}_N\\ 0\end{bmatrix}\\ &= \frac{3Hc_3p_n^2}{2W^2}\left(\frac{\phi_c}{W}-1\right)\begin{bmatrix}0_{2N+1}^{\mathrm{T}}\\ E^{-1/2}T\end{bmatrix}\bar{e}_N\\ &= \frac{3Hc_3p_n^2}{2W^2}\sqrt{\frac{2N+1}{l_c}}\left(\frac{\phi_c}{W}-1\right)\begin{bmatrix}0\\ e_N\end{bmatrix}. \end{aligned} \tag{41}$$

By $SQ_0[r_n, \bar{r}_n] = -2DS\mu_n$ with $\gamma = \gamma_c$,

$$\begin{aligned} \mu_n &= -\frac{3Hc_3p_n^2}{4W^2}\sqrt{\frac{2N+1}{l_c}}\left(\frac{\phi_c}{W}-1\right)S^{-1}D^{-1}\begin{bmatrix}0\\ e_N\end{bmatrix}\\ &= -\frac{3Hc_3p_n^2}{4W^2}\sqrt{\frac{2N+1}{l_c}}\left(\frac{\phi_c}{W}-1\right)\begin{bmatrix}0_{2N+1} & T^{\mathrm{T}}E^{-1/2}e_N\\ \frac{1}{2B\sqrt{(2N+1)l_c}} & 0\end{bmatrix}D_0^{-1}\begin{bmatrix}0\\ 1\end{bmatrix}\\ &= -\frac{3Hc_3p_n^2}{4W^2l_c}\left(\frac{\phi_c}{W}-1\right)\begin{bmatrix}0_{2N+1} & \bar{e}_N\\ \frac{1}{2B} & 0\end{bmatrix}D_0^{-1}\begin{bmatrix}0\\ 1\end{bmatrix}. \end{aligned} \tag{42}$$

Using the expression for $D_0$, we obtain

$$D_0^{-1} = \begin{bmatrix}\tau & \kappa\\ -\kappa & \alpha/l_c\end{bmatrix}^{-1} = \frac{1}{\kappa^2+\alpha\tau/l_c}\begin{bmatrix}\alpha/l_c & -\kappa\\ \kappa & \tau\end{bmatrix},\quad \alpha = 0. \tag{43}$$

It follows that

$$\mu_n = -\frac{3Hc_3p_n^2}{4W^2(\kappa^2l_c+\alpha\tau)}\left(\frac{\phi_e}{W}-1\right)\begin{bmatrix}\tau\bar{e}_N\\ \frac{-\kappa}{2B}\end{bmatrix},\quad \alpha = 0. \tag{44}$$

The computation of the vector $\nu_n$, which is more complicated, is summarized in the next result.

**Lemma 3.2.** *The vector $\nu_n$ as defined in (75) for the local multimode model is given by*

$$\nu_n = \frac{3Hc_3 p_n^2(\omega_{2n} + 2\omega_n + \alpha_{2n} j) j e^{j2\delta_n}}{4m_{2n} W^2(\omega_{2n}^2 - 4\omega_n^2 + \alpha_{2n}^2 - 2\alpha_{2n}\omega_n j)} \left(\frac{\phi_c}{W} - 1\right) \begin{bmatrix} \Theta_{2n} \\ 0 \end{bmatrix}, \tag{45}$$

*where $1 \le n \le N/2$, and $\alpha_{2n} = \left(\alpha - \mu(2n)^2\right) m_{2n}^{-1}$. For $N < 2n \le 2N$, $\nu_n$ has the same expression as in (45) except that $2n$ is replaced by $\eta = 2(N-n)+1$, and $\Theta_{2n}$ by $\Theta_{-\eta}$.*

**Proof.** See the Appendix. □

The next result gives the stability condition for each projected dynamics along the $n$th pair of the critical eigenvectors.

**Theorem 3.3.** *For $0 < 2n \le N$, the stability characteristic value (SCV) for the nth pair of critical modes corresponding to rotating stall is given by*

$$\tilde{\lambda}_2^{(n)} = \frac{3Hc_3 p_n^2}{m_n W^4} \left[ \frac{W}{4} + \left(\frac{\phi_c}{W} - 1\right)^2 \left( \frac{\Omega_\omega^{\alpha,n}}{2} - \frac{3H\tau c_3}{\kappa^2 l_c + \alpha\tau} \right) \right] \tag{46}$$

$$\Omega_\omega^{\alpha,n} = \frac{3Hc_3}{m_{2n}} \cdot \frac{\alpha_{2n}\omega_{2n}^2 + \alpha_{2n}^3 + 2\alpha_{2n}\omega_n\omega_{2n}}{(\omega_{2n}^2 - 4\omega_n^2 + \alpha_{2n}^2)^2 + 4\alpha_{2n}^2\omega_n^2}, \tag{47}$$

*where $\omega_n = \frac{n}{b} m_n^{-1}$. For $N < 2n \le 2N$, $\tilde{\lambda}_2^{(n)}$ is the same as in (46) except that $2n$ is replaced by $\eta = 2(N-n)+1$.*

**Proof.** It is straightforward to obtain

$$\ell_n Q[x, y] = \frac{3Hc_3}{m_n W^2} \left(\frac{\phi_c}{W} - 1\right) \ell_n(x \cdot y), \tag{48}$$

$$\ell_n C[x, y, z] = \frac{Hc_3}{m_n W^3} \ell_n(x \cdot y \cdot z). \tag{49}$$

With $\mu_n$ and $\nu_n$ obtained as in (44) and (45), we have

$$r_n \cdot \mu_n = -\frac{3Hc_3\tau p_n^2 r_n}{4W^2(\kappa^2 l_c + \alpha\tau)} \left(\frac{\phi_c}{W} - 1\right), \tag{50}$$

$$\bar{r}_n \cdot \nu_n = \frac{3Hc_3}{m_{2n}} \cdot \frac{p_n^2(\omega_{2n} + 2\omega_n + \alpha_{2n} j) j r_n}{4W^2(\omega_{2n}^2 - 4\omega_n^2 + \alpha_{2n}^2 - 2\alpha_{2n}\omega_n j)} \left(\frac{\phi_c}{W} - 1\right). \tag{51}$$

If $2n > N$, $2n$ should be replaced by $-\eta = -(2N + 1 - 2n)$ in (51). Now

$$\mathrm{Re}\,[\ell_n(r_n \cdot \mu_n)] = -\frac{3Hc_3\tau p_n^2}{4W^2(\kappa^2 l_c + \alpha\tau)} \left(\frac{\phi_c}{W} - 1\right),$$

$$\mathrm{Re}\,[\ell_n(r_n \cdot \bar{r}_n \cdot r_n)] = \frac{p_n^2}{2}, \tag{52}$$

$$\mathrm{Re}\,[\ell_n(\bar{r}_n \cdot \nu_n)] = \frac{3\Omega_\omega^{\alpha,n} H c_3 p_n^2}{4m_{2n} W^2} \left(\frac{\phi_c}{W} - 1\right), \tag{53}$$

$$\Omega_\omega^{\alpha,n} = \mathrm{Im}\left[\frac{(\omega_{2n} + 2\omega_n + \alpha_{2n} j)/m_{2n}}{\omega_{2n}^2 - 4\omega_n^2 + \alpha_{2n}^2 - 2\alpha_{2n}\omega_n j}\right]. \tag{54}$$

Hence the expression for $\tilde{\lambda}_2^{(n)}$ in (46) can be verified following (76). □

As mentioned earlier, $\tilde{\lambda}_2^{(n)} < 0$ for $n = 1, 2, \ldots, N$ may not imply stability of the rotating stall dynamics because of the coupling between different pairs of the critical modes. However for the special case of $\mu = 0$ (that is, when $N$ pairs of the critical modes in (30) cross the imaginary axis simultaneously), $\tilde{\lambda}_2^{(n)} < 0$ for $n = 1, 2, \ldots, N$ determines the stability of the rotating stall dynamics, which is surprising. The next lemma gives the expressions of $\mu_{n_l}$ and $\nu_{n_l}$ as in (79), which will be useful in establishing the final result of our paper. The derivations of $\mu_{n_l}$ and $\nu_{n_l}$ are similar to those of $\mu_n$ and $\nu_n$, so the proof is omitted.

**Lemma 3.4.** *Suppose that $\mu = 0$. Then the vectors $\mu_{n_l}$ and $\nu_{n_l}$ as defined in (79) for the local compression model are given by*

$$\mu_{n_l} = \frac{3Hc_3 p_n p_l j e^{j(\delta_n - \delta_l)}}{4m_{|n-l|} W^2 (\omega_{|n-l|} - \omega_n + \omega_l)} \left(\frac{\phi_c}{W} - 1\right) \begin{bmatrix} \Theta_{n-l} \\ 0 \end{bmatrix}, \tag{55}$$

$$\nu_{n_l} = \begin{cases} \dfrac{3Hc_3 p_n p_l j e^{j(\delta_n + \delta_l)}}{4m_{n+l} W^2 (\omega_{n+l} - \omega_n - \omega_l)} \left(\dfrac{\phi_c}{W} - 1\right) \begin{bmatrix} \Theta_{n+l} \\ 0 \end{bmatrix}, & 0 < n + l \le N, \\ \dfrac{3Hc_3 p_n p_l j e^{j(\delta_n + \delta_l)}}{4m_\eta W^2 (\omega_\eta - \omega_n - \omega_l)} \left(\dfrac{\phi_c}{W} - 1\right) \begin{bmatrix} \Theta_{-\eta} \\ 0 \end{bmatrix}, & N < n + l \le 2N, \end{cases} \tag{56}$$

*where $n, l = 1, 2, \ldots, N$, $n \neq l$, $\eta = 2N + 1 - n - l$, $\phi_c$ is as in (36), and $\Theta_n$ is as in (37).*

**Theorem 3.5.** *Under the conditions $\mu = 0$, $c_3 < 0$, and $c_1 + 3c_3 = 0$, the rotating stall dynamics are locally stable if and only if $c_0 + 10c_3 > 0$.*

**Proof.** Local stability of rotating stall implies that each pair of the corresponding critical modes is locally stable, which implies that $\tilde{\lambda}_2^{(n)} < 0$ for $n = 1, 2, \ldots, N$. Because $\phi_c = 2W$, $\mu = 0$, and $\alpha = 0$ at the criticality, $\alpha_{2n} = 0$ for $1 \le n \le N$. It follows that for $n = 1, 2, \ldots, N$, $\tilde{\lambda}_2^{(n)} < 0$ is equivalent to

$$\frac{3Hc_3 p_n^2}{W^3} \left(\frac{1}{4} - \frac{3H\tau c_3}{W l_c \kappa^2}\right) < 0. \tag{57}$$

Because $c_3 < 0$ and all other parameters are positive, this relation is equivalent to

$$\frac{1}{4} - \frac{3H\tau c_3}{W l_c \kappa^2} > 0. \tag{58}$$

Noting that the expression of $\tau$ at criticality becomes

$$\tau = -\frac{W}{4B^2 H l_c (c_0 + c_1 + c_3)}, \tag{59}$$

straightforward calculation proves that $\tilde{\lambda}_2^{(n)} < 0$ is equivalent to $c_0 + 10c_3 > 0$.

For sufficiency, assume that $c_0 + 10c_3 > 0$, which is equivalent to $\tilde{\lambda}_2^{(n)} < 0$ for $n = 1, 2, \ldots, N$. It will be shown using Theorem 5.3 that the compressor model is locally stable at uniform flow equilibrium $\phi_e = \phi_c$, and $\psi_e = \psi_c$ with $\gamma = \gamma_c$. Indeed there holds $\chi_{nn} = 8\tilde{\lambda}_2^{(n)} < 0$ for $n = 1, 2, \ldots, N$. Furthermore, through straightforward calculations,

$$\ell_n(\bar{r}_l \cdot \nu_{n_l}) = j r_\nu \frac{m_n p_n^2 p_l^2}{8}(2N + 1), \tag{60}$$

$$\ell_n(r_l \cdot \mu_{n_l}) = j r_\mu \frac{m_n p_n^2 p_l^2}{8}(2N + 1), \tag{61}$$

for $n \neq l$ where $r_\mu, r_\nu$ are real numbers. Thus

$$\mathrm{Re}\left[\ell_n(r_l \cdot \mu_{n_l})\right] = \mathrm{Re}\left[\ell_n(\bar{r}_l \cdot \nu_{n_l})\right] = 0 \tag{62}$$

for $n, l = 1, 2, \ldots, N$. It follows that

$$\chi_{nl} = 16\mathrm{Re}\left(\ell_n Q[r_n, \mu_l] + \frac{3}{4}\ell_n C[r_n, r_l, \bar{r}_l]\right) \tag{63}$$

at $\gamma = \gamma_c$. Using the expression of $r_n$, and $\phi_c = 2W$,

$$r_n \cdot \mu_l = -\frac{3Hc_3 \tau p_l^2}{4W^2 \kappa^2 l_c} r_n, \quad r_n \cdot r_l \cdot \bar{r}_l = \frac{p_l^2}{2} r_n. \tag{64}$$

By (48), (49), and relation $\ell_n r_n = 1$,

$$\ell_n Q[r_n, \mu_l] = -\frac{\tau}{m_n l_c}\left(\frac{3Hc_3 p_l}{2W^2 \kappa}\right)^2, \quad \ell_n C[r_n \cdot r_l \cdot \bar{r}_l] = \frac{Hc_3 p_l^2}{2m_n W^3}. \tag{65}$$

The expression of $\chi_{nl}$ is then obtained as

$$\chi_{nl} = \frac{12Hc_3 p_l^2}{m_n W^3}\left(\frac{1}{2} - \frac{3H\tau c_3}{W l_c \kappa^2}\right). \tag{66}$$

Again, because $c_3 < 0$ and all other parameters are positive, $\chi_{nl} \leq 0$ is equivalent to

$$\frac{1}{2} - \frac{3H\tau c_3}{W l_c \kappa^2} \geq 0, \tag{67}$$

which is implied by (58). Hence the bifurcated system is locally stable in light of Theorem 5.3. □

It is very surprising to see that the stability condition for rotating stall is identical to the case of $N = 1$ for the third-order Moore-Greitzer model [9]. However, it should be noted that the result of Theorem 5.3 is derived based on assumptions that $\mu = 0$, and $\psi_c(\cdot)$ is cubic satisfying $c_3 < 0$ and $c_1 + 3c_3 = 0$ as in [10], [9].

## 4. Conclusion

Rotating stall dynamics were investigated in this paper for axial flow compressors, and necessary and sufficient conditions were obtained for local stability of the rotating stall dynamics in terms of various compressor parameters. Although our stability conditions were derived for the multimode Moore-Greitzer model, they hold for the limiting case, i.e., the full PDE Moore-Greitzer model. This result is important because past research has almost exclusively focused on the third-order Moore-Greitzer model ($N = 1$), of which many active control laws were proved to be effective in the literature but fail to work in engineering practice because of the spillover of the high-order modes [4]. Our local stability conditions clearly offer new insight into the design and active control of rotating stall for the multimode Moore-Greitzer model, thereby improving the performance of axial flow compressors.

## 5. Appendix

This section reviews briefly the projection and Lyapunov methods for local stability analysis of Hopf bifurcations and gives some of the proofs for Section 3.

For stability analysis of Hopf bifurcations, the system under consideration is the following $n$th-order parameterized nonlinear system:

$$\dot{x} = f(\gamma, x), \quad f(\gamma, 0) = 0 \ \forall \gamma \in \mathbf{R} \ \text{ and } \ x_0 \in \mathcal{S} \subset \mathbf{R}^n, \tag{68}$$

where $x \in \mathbf{R}^n$, $\gamma$ is a real-valued parameter, and $\mathcal{S}$ is a linear subspace of $\mathbf{R}^n$, to be clarified later. It is assumed that $f(\cdot, \cdot)$ is sufficiently smooth such that the equilibrium solution $x_e$, satisfying $f(\gamma, x_e) = 0$, is a smooth function of $\gamma$. The smoothness of $f(\cdot, \cdot)$ implies the existence of a Taylor series expansion near the origin of $\mathbf{R}^n$ in the form

$$\dot{x} = f(\gamma, x) = L(\gamma)x + Q(\gamma)[x, x] + C(\gamma)[x, x, x] + \cdots, \tag{69}$$

where $L(\gamma)x$, $Q(\gamma)[x, x]$, and $C(\gamma)[x, x, x]$ can be expanded into

$$L(\gamma)x = L_0 x + \delta\gamma L_1 x + \delta\gamma^2 L_2 x + \cdots, \tag{70}$$

$$Q(\gamma)[x, x] = Q_0[x, x] + \delta\gamma Q_1[x, x] + \cdots, \tag{71}$$

$$C(\gamma)[x, x, x] = C_0[x, x, x] + \delta\gamma C_1[x, x, x] + \cdots, \tag{72}$$

with $\delta\gamma = \gamma - \gamma_c$, and $L_0$, $L_1$, $L_2$ constant matrices of size $(n \times n)$. Suppose that $L(\gamma)$ possesses $m$ ($\leq n/2$) pairs of complex eigenvalues $\lambda_k(\gamma) = \alpha_k(\gamma) \pm j\beta_k(\gamma)$, dependent smoothly on $\gamma$. It is assumed that for $1 \leq k \leq m$,

$$\alpha_k(\gamma_c) = 0, \quad \beta(\gamma_c) = \omega_k \neq 0, \quad \alpha_k'(\gamma_c) = \frac{d\alpha_k}{d\gamma}(\gamma_c) \neq 0, \tag{73}$$

while all other eigenvalues of $L(\gamma)$ are stable at and in a neighborhood of $\gamma = \gamma_c$. That is, $m$ pairs of eigenvalues cross the imaginary axis simultaneously. Then each

$\lambda_k(\gamma)$ is a critical eigenvalue, and so is its conjugate. The center space, or the eigenspace, for the $m$ pairs of critical eigenvalues is denoted by $\mathcal{S}_c$, and is assumed to be orthogonally complementary to $\mathcal{S}$ in the sense that $\mathcal{S} \oplus \mathcal{S}_c = \mathbf{R}^n$. Because the projection of $x_0 \in \mathcal{S}$ to $\mathcal{S}_c$ is zero, the equilibrium $x_0$ satisfying (68) will be called the zero solution. The strict crossing assumption implies that the zero solution changes its stability as $\gamma$ crosses $\gamma_c$. For instance, $\alpha_k'(\gamma_c) > 0$ implies that the zero solution is locally stable for $\gamma < \gamma_c$ and becomes unstable for $\gamma > \gamma_c$. The crucial problem is the determination of local stability near the critical parameter $\gamma_c$ at which Hopf bifurcations occur and the periodic solutions are born.

### *A.1. The projection method.*

The center space $\mathcal{S}_c$, spanned by all the critical eigenvectors, is complete. If all the critical eigenvalues are distinct, then

$$\mathcal{S}_c = \mathcal{S}_{c_1} \oplus \mathcal{S}_{c_2} \oplus \cdots \oplus \mathcal{S}_{c_m}, \tag{74}$$

where $\mathcal{S}_{c_k}$ denotes the eigenspace spanned by the $k$th pair of the critical eigenvectors. The projection method in [7] projects the nonlinear dynamics into the subspace of $\mathcal{S}_{c_k}$ so that stability of the projected dynamics can be analyzed. Associated with each pair of the critical eigenvalues $(\lambda_k, \bar{\lambda}_k)$, there can define an SCV (stability characteristic value) $\tilde{\lambda}_2^{(k)}$ whose sign determines local stability of the projected dynamics. See [7], [6], [1] for details. Let the Taylor series of $f(\gamma, x)$ be of the form in (69), where $L_0 = L(0)$. An algorithm to compute $\tilde{\lambda}_2^{(k)}$ is now outlined.

Step 1. Compute the left row eigenvector $\ell_k$ and the right column eigenvector $r_k$ of $L_0$ corresponding to the $k$th critical eigenvalue of $\lambda_k(0) = j\omega_k$. Normalize by setting $\ell_k r_k = 1$.

Step 2. Solve column vectors $\mu_k$ and $\nu_k$ from the equations

$$-L_0\mu_k = \frac{1}{2}Q_0[r_k, \bar{r}_k], \quad (2j\omega_k I - L_0)\nu_k = \frac{1}{2}Q_0[r_k, r_k]. \tag{75}$$

Step 3. The coefficient $\tilde{\lambda}_2^{(k)}$ is given by

$$\tilde{\lambda}_2^{(k)} = 2\mathrm{Re}\left\{2\ell_k Q_0[r_k, \mu_k] + \ell_k Q_0[\bar{r}_k, \nu_k] + \frac{3}{4}\ell_k C_0[r_k, r_k, \bar{r}_k]\right\}. \tag{76}$$

**Theorem 5.1.** *Suppose that $L_0$ has $N$ pairs of nonzero critical eigenvalues on the imaginary axis with the rest on the open left half-plane. Then the projected dynamics along the $k$th pair of the eigenvectors is stable if $\tilde{\lambda}_2 < 0$, and unstable if $\tilde{\lambda}_2 > 0$. For the case of $N = 1$, the associated Hopf bifurcation is supercritical or stable if $\tilde{\lambda}_2 < 0$, and subcritical or unstable if $\tilde{\lambda}_2 > 0$.*

It should be clear that if $L_0$ admits only a single pair of imaginary eigenvalues, then local stability of the bifurcated system is equivalent to $\tilde{\lambda}_2^{(k)} < 0$. However, if $L_0$ admits more than one pair of imaginary eigenvalues, local stability of each projected dynamics does not guarantee local stability of the bifurcated systems. In this case, local stability of the bifurcated systems can be tackled by the Lyapunov method [3].

### *A.2. The Lyapunov method.*

The Lyapunov method for multiple critical modes has been developed by Fu [3]. The method gives sufficient conditions on the existence of the Lyapunov function to guarantee local stability of the bifurcated system. The following notion is needed.

**Definition 5.2.** Under the condition that $L_0$ admits $N > 1$ pairs of eigenvalues on the imaginary axis with the rest on the open left half-plane, the nonlinear system (69) is said to be locally center-symmetric in the sense of Lyapunov if the following conditions hold:

$$\begin{array}{llll} \omega_i \neq \omega_m, & \omega_i \neq 2\omega_m & \omega_i \neq 3\omega_m & \text{whenever } N \geq 2, \\ \omega_i \neq \omega_m + \omega_k, & \omega_i \neq 2\omega_m + \omega_k, & 2\omega_i \neq \omega_m + \omega_k, & \text{whenever } N \geq 3, \\ \omega_i \neq \omega_m + \omega_k + \omega_l, & \omega_i + \omega_m \neq \omega_k + \omega_l, & & \text{whenever } N \geq 4, \end{array}$$

hold where all indices are distinct.

**Theorem 5.3.** *Suppose that $L_0$ admits $N > 1$ pairs of eigenvalues on the imaginary axis with the rest on the open left half-plane, and the nonlinear system (69) is locally center-symmetric in the sense of Lyapunov. Then there exists a Lyapunov function that guarantees local stability of (69) at the criticality if*

$$\chi_{kk} = 16\mathrm{Re}\left\{\ell_k\left(2Q_0[r_k, \mu_k] + Q_0[\bar{r}_k, \nu_k] + \frac{3}{4}C_0[r_k, r_k, \bar{r}_k]\right)\right\} < 0, \quad \text{for } k = 1, \cdots, N, \tag{77}$$

$$\chi_{kp} = 16\mathrm{Re}\left\{\ell_k\left(Q_0[r_k, \mu_p] + Q_0[\bar{r}_p, \nu_{k_p}] + Q_0[r_p, \mu_{k_p}] + \frac{3}{4}C_0[r_k, r_p, \bar{r}_p]\right)\right\} \leq 0, \tag{78}$$

*for $k, p = 1, \ldots, N$ with $k \neq p$, where $\mu_k$, $\nu_k$ are the solutions to (75), and $\mu_{k_p}$, $\nu_{k_p}$ are given by*

$$\begin{aligned} \mu_{k_p} &= -\frac{1}{2}(L_0 - j(\omega_k - \omega_p))^{-1} Q_0[r_k, \bar{r}_p], \\ \nu_{k_p} &= -\frac{1}{2}(L_0 - j(\omega_k + \omega_p))^{-1} Q_0[r_k, r_p]. \end{aligned} \tag{79}$$

It is noted that $\chi_{kk} = 8\tilde{\lambda}_2^{(k)}$. Hence local stability of Hopf bifurcations with multiple pairs of critical modes requires more than local stability of each projected dynamics. Roughly speaking, the nonpositivity of $\chi_{kp}$ with $k \neq p$ takes the coupling of different pairs of critical modes into account for local stability of the bifurcated system in (69).

### *A.3. Proof of Lemma 3.1.*

Note that $D = SLS^{-1}$ as in (27). If $r_D$ is an eigenvector of $D$, then $S^{-1}r_D$ is an eigenvector of $L$. Let the $n$th eigenvector of $D$ be denoted by $x_n + jy_n$ where $x_n$ and $y_n$ are real vectors of size $2(N+1)$ corresponding to the eigenvalue of $j\omega_n$ at $\gamma = \gamma_c$ where $\omega_n = n/(bm_n) > 0$ for $n = 1, 2, \ldots, N$. By equating real and imaginary parts of the eigenequation for $D$, the two equations

$$Dx_n = -\omega_n y_n, \quad Dy_n = \omega_n x_n, \tag{80}$$

are obtained. This yields the eigenequations

$$D^2 x_n = -\omega_n^2 x_n, \quad D^2 y_n = -\omega_n^2 y_n. \tag{81}$$

Hence $x_n$ and $y_n$ satisfy the same eigenequation. We need to solve only one of them; the other can be obtained from either $Dx_n = -\omega_n y_n$ or $Dy_n = \omega_n x_n$. At $\gamma = \gamma_c$,

$$D^2 = \mathrm{diag}(D_0^2, D_1^2, \ldots, D_N^2), \quad D_n^2 = -\omega_n^2 I_2, \quad n = 1, 2, \ldots, N. \tag{82}$$

Thus it follows that the $(2 \times 2)$ matrix $D_n$ at the $(n+1)$th diagonal block of $D^2$ is canceled in the sum of $D^2 + \omega_n^2 I$. Because $(D^2 - \omega_n^2 I)x_n = 0$, and $\det(D_0^2) = (\kappa^2 + \tau\alpha/l_c)^2 \neq 0$, $x_n$ has the form

$$x_n = [\, 0_{2n} \quad u_n^{\mathrm{T}} \quad 0_{2(N-n)} \,]^{\mathrm{T}}, \quad 0_{2k} \in \mathbf{R}^{2k}, \tag{83}$$

where $u_n$ is an arbitrary nonzero real column vector of size 2. Now $y_n$ can be calculated as

$$y_n = -\frac{1}{\omega_n} Dx_n = -\frac{1}{\omega_n} [\, 0_{2n} \quad (D_n u_n)^{\mathrm{T}} \quad 0_{2(N-n)} \,]^{\mathrm{T}} = [\, 0_{2n} \quad v_n^{\mathrm{T}} \quad 0_{2(N-n)} \,]^{\mathrm{T}}. \tag{84}$$

The right eigenvector $r_n$ corresponding to the eigenvalue $j\omega_n$ is thus given by

$$r_n = S^{-1}(x_n + jy_n) = S^{-1} \begin{bmatrix} 0_{2n} \\ u_n + jv_n \\ 0_{2(N-n)} \end{bmatrix}, \quad v_n = \begin{bmatrix} 0 & 1 \\ -1 & 0 \end{bmatrix} u_n, \tag{85}$$

for $n = 1, 2, \ldots, N$. The relation between $u_n$ and $v_n$ implies that

$$u_n + jv_n = Ju_n, \quad J = \begin{bmatrix} 1 & j \\ -j & 1 \end{bmatrix} = \begin{bmatrix} 1 \\ -j \end{bmatrix} [\, 1 \quad j \,], \tag{86}$$

where $n = 1, 2, \ldots, N$. It is now clear that

$$r_n = \begin{bmatrix} 0_{2N+1} & T^{\mathrm{T}}E^{-1/2} \\ (2B\sqrt{(2N+1)l_c})^{-1} & 0_{2N+1}^{\mathrm{T}} \end{bmatrix} \begin{bmatrix} 0_{2n} \\ u_n + jv_n \\ 0_{2(N-n-1)} \end{bmatrix}$$
$$= \sqrt{\frac{2m_n^{-1}}{2N+1}} \begin{bmatrix} \cos n\theta_1 & \sin n\theta_1 \\ \vdots & \vdots \\ \cos n\theta_{2N+1} & \sin n\theta_{(2N+1)} \\ 0 & 0 \end{bmatrix} (u_n + jv_n), \tag{87}$$

which becomes the same as (38) by substituting the expression of $u_n + jv_n$ as in (86). Next denote $\ell_D$ as the left eigenvector of $D$. Because of the block structure of $D$ and $D_n = -D_n^T$ at $\gamma = \gamma_c$ for $n = 1, 2, \ldots, N$, $\ell_D = r_D^{\mathrm{H}}$. Hence

$$\ell_n = \ell_D S = r_D^{\mathrm{H}} S = r_n^{\mathrm{H}} S^{\mathrm{H}} S = r_n^{\mathrm{H}} \begin{bmatrix} T^{\mathrm{T}}ET & 0_{2N+1} \\ 0_{2N+1}^{\mathrm{T}} & 4B^2 l_c(2N+1) \end{bmatrix} = r_n^{\mathrm{H}} m_n, \tag{88}$$

which gives the expression of $\ell_n$. The normalization condition $\ell_n r_n = 1$ yields

$$\ell_n r_n = m_n r_n^{\mathrm{H}} r_n = 2\|u_n\|^2 = 1, \tag{89}$$

which is equivalent to $\|u_n\| = 1/\sqrt{2}$. The proof is now complete.

### *A.4. Proof of Lemma 3.2.*

By definition in (75),

$$\nu_n = \frac{1}{2}(2j\omega_n - L_0)^{-1} Q_0[r_n, r_n] = \frac{1}{2} S^{-1}(2j\omega_n - D)^{-1} S Q_0[r_n, r_n]$$
$$= \frac{p_n^2}{4} S^{-1}(2j\omega_n - D)^{-1} S \begin{bmatrix} \frac{3Hc_3}{W^2}\left(\frac{\phi_e}{W} - 1\right) T^{\mathrm{T}}E^{-1}T & 0_{2N+1} \\ 0_{2N+1}^{\mathrm{T}} & -\frac{\tau}{4\Psi_c} \end{bmatrix} \begin{bmatrix} \Theta_{2n} \\ 0 \end{bmatrix} e^{j2\delta_n}. \tag{90}$$

There are two cases to consider:

(i) $2n \le N$

(ii) $N < 2n \le 2N$.

For (i),

$$\nu_n = \frac{3Hc_3 p_n^2 e^{j2\delta_n}}{4m_{2n}W^2}\left(\frac{\phi_c}{W} - 1\right) S^{-1}(2j\omega_n - D)^{-1} S \begin{bmatrix} \Theta_{2n} \\ 0 \end{bmatrix}$$
$$= \frac{3Hc_3 p_n^2 e^{j2\delta_n}}{4m_{2n}W^2}\left(\frac{\phi_c}{W} - 1\right) \begin{bmatrix} \cos(2n\theta_1) & \sin(2n\theta_1) \\ \vdots & \vdots \\ \cos(2n\theta_{2N+1}) & \sin(2n\theta_{2N+1}) \\ 0 & 0 \end{bmatrix}$$

$$\times\ (2j\omega_n - D_{2n})^{-1}\begin{bmatrix} 1 \\ -j \end{bmatrix}. \tag{91}$$

At the critical parameter $\gamma = \gamma_c$,

$$D_n = \begin{bmatrix} 0 & -\omega_n \\ \omega_n & 0 \end{bmatrix}\ ,\quad \omega_n = \frac{n}{b}m_n^{-1}. \tag{92}$$

Then straightforward computation gives

$$(2j\omega_n - D_{2n})^{-1}\begin{bmatrix} 1 \\ -j \end{bmatrix} = \frac{(\omega_{2n} + 2\omega_n + \alpha_{2n}j)j}{\omega_{2n}^2 - 4\omega_n^2 + \alpha_{2n}^2 - 2\alpha_{2n}\omega_n j}\begin{bmatrix} 1 \\ -j \end{bmatrix}. \tag{93}$$

Hence for $n \le N/2$, direct computation gives the expression in (45).

For (ii), without loss of generality, it is assumed that $\theta_k = 2(k-1)\pi/(2N+1)$, where $1 \le k \le 2N+1$. Because $N < 2n \le 2N$,

$$2n = 2N + 1 - \eta,\quad 0 < \eta \le N. \tag{94}$$

It follows that for $1 \le k \le 2N+1$,

$$e^{-j2n\theta_k} = e^{-j(2N+1-\eta)\theta_k} = e^{j\eta\theta_k}, \tag{95}$$

where $0 < \eta \le N$. In this case,

$$\nu_n = \frac{3Hc_3p_n^2e^{j2\delta_n}}{4m_\eta W^2}\left(\frac{\phi_c}{W} - 1\right)S^{-1}(2j\omega_n - D)^{-1}S\begin{bmatrix} \Theta_{-\eta} \\ 0 \end{bmatrix}. \tag{96}$$

Noticing that

$$(2j\omega_n - D_\eta)^{-1} = \frac{1}{\omega_\eta^2 - 4\omega_n^2 + \alpha_\eta^2 - 2\alpha_\eta\omega_n j}\begin{bmatrix} 2j\omega_n - \alpha_\eta & -\omega_\eta \\ \omega_\eta & 2j\omega_n - \alpha_\eta \end{bmatrix}, \tag{97}$$

$$(2j\omega_n - D_\eta)^{-1}\begin{bmatrix} 1 \\ j \end{bmatrix} = \frac{(\omega_\eta + 2\omega_n + \alpha_\eta j)j}{\omega_\eta^2 - 4\omega_n^2 + \alpha_\eta^2 - 2\alpha_\eta\omega_n j}\begin{bmatrix} 1 \\ j \end{bmatrix}, \tag{98}$$

direction computation gives the same $\nu_n$ as in (45) except that $2n$ is replaced by $-\eta$ with $\omega_{-\eta} = \omega_\eta$, $\alpha_{-\eta} = \alpha_\eta$, and $m_{-\eta} = m_\eta$.

## References


[1] E. H. Abed and Jyun-Horng Fu, Local feedback stabilization and bifurcation control, I — Hopf bifurcation, *Systems Control Lett.*, 7, 11–17, 1986.

[2] R. A. Adomaitis and E. H. Abed, Bifurcation analysis of nonuniform flow patterns in axial-flow gas compressors, *1st World Congress of Nonlinear Analysis*, Aug. 1992.

[3] J.-H. Fu, Lyapunov functions and stability criteria for nonlinear systems with multiple critical modes, *Math. Control Signals Systems*, 7, 255–278, 1994.

[4] G. Gu, S. Banda, and A. Sparks, An overview of rotating stall and surge control for axial flow compressors, *Proc. 35th IEEE Conf. on Dec. and Contr.*, Kobe, Japan, 2786–2791, Dec. 1996.

[5] R. A. Horn and C. R. Johnson, *Topics in Matrix Analysis*, Cambridge University Press, London and New York, 1991.

[6] L. N. Howard, Nonlinear oscillations, in F. C. Hoppensteadt, ed., *Nonlinear Oscillations in Biology*, American Mathematical Society, Providence, RI, 1979, pp. 1–68.

[7] G. Iooss and D. D. Joseph, *Elementary Stability and Bifurcation Theory*, Springer-Verlag, Berlin and New York, 1980.

[8] C. A. Mansoux, J. D. Setiawan, D. L. Gysling, and J. D. Paduano, Distributed nonlinear modeling and stability analysis of axial compressor stall and surge, *Proc. 1994 Amer. Contr. Conf.*, 2305–2316, 1994.

[9] F. E. McCaughan, Bifurcation analysis of axial flow compressor stability, *SIAM J. Appl. Math.*, vol. 20, 1232–1253, 1990.

[10] F. K. Moore and E. M. Greitzer, A theory of post-stall transients in axial compressors, Part I — Development of the equations, *ASME J. of Engrg. Gas Turbines and Power*, vol. 108, 68–76, 1986.